NIPPON STEEL TECHNICAL REPORT No. 102 JANUARY 2013

Technical Report

UDC 621 . 774 . 2 : 539 . 4 . 072

Forming and Buckling Simulation on High-strength UOE Pipe with Plastic Anisotropy

Eiji TSURU*
Yukinobu NAGATA
Yasuhiro SHINOHARA
Jun AGATA
Satoshi SHIRAKAMI

Abstract

New guideline is required in forming high strength steel line pipes since spring-back is quite higher than that of the conventional materials. Moreover, line pipes have plastic anisotropy, which the work hardening coefficients are different between the longitudinal and the circumferential direction, caused by the forming strain and the strain aging during the heating in anti-corrosion coating. However, the effect of the plastic anisotropy on the pipe performance has not been clarified. This paper describes the numerical simulation models of the UOE pipe forming and the pipe bending with two different yield functions, which are capable of representing the plastic hysteresis and the orthogonal anisotropy respectively. The forming models introduce the operating guidelines corresponding to the material strength and the design indexes of the apparatus to aid the lack of the press capacity. The bending models reveal that yield point elongation on stress vs. strain curve in the circumferential direction in addition to the longitudinal direction degrades the buckling resistance and the decreasing rate is dependent on internal pressure.

1. Introduction

A UOE pipe is used for long-distance pipelines to transport natural gas and crude oil. In recent years, the demand for high-strength steels for a UOE pipe, from X80 to X120, has been increasing since they help cut the cost of transportation. Many of those high-strength UOE pipes are thin-walled; that is, they have a large D/t ratio (D: outside diameter, t: wall thickness). Besides, they require special attention to the spring back of the steel plate and the press capacity used in the pipe-forming process. On the other hand, more and more pipelines have been laid in districts, which are subject to hostile natural conditions. Pipelines embedded in discontinuous permafrost regions undergo repetitions of thawing and frost heaving of the permafrost. As a result, steel pipes may suffer flexural deformation under internal pressures far in excess of their yield strength. The design technique that considers such plastic deformation is called strain-based design (SBD). Line pipes are required to have a high degree of deformability.

In the development of line pipes that meet the market needs described above, numerical simulations are applied as one of the important analytical techniques. This report describes the results of our numerical simulation of a UOE pipe forming by finite element analy-

* Chief Researcher, Dr.Eng., Plate, Pipe, Tube & Shape Research Lab., Steel Research Laboratories
20-1, Shintomi, Futtsu, Chiba 293-8511

sis (FEA) and our analysis of the deformation behavior of a UOE pipe that has orthogonal anisotropy. In the simulation of UOE pipe forming, we applied the material hardening law that accurately permits the prediction of the spring back and proposed a method of creating a simple model of the rigidity of press housing that can be used in the actual production of a UOE pipe. In the analysis of flexural buckling behavior, by using a newly developed material-hardening law that considers the orthogonal anisotropy of steel pipe, we improved the prediction accuracy of the critical buckling strain and clarified the influence of the mechanical properties of pipes in the circumferential (C) direction on the buckling limit.

2. UOE Pipe-forming Process and Its Working Environment

2.1 UOE pipe-forming process

Fig. 1 schematically presents a typical process for forming a UOE pipe. The stock plate is subjected to cold working by a C-press, a U-press, an O-press, a seam welding, and an expander in that order. The C-press bends each of the two previously beveled edges of the plate by pinching it with the curved upper and lower dies. The Burson-type U-press subjects the central part of the plate to three-point bending using a U-punch and forms the plate into a U shape with auxiliary forming dies called rocking dies. The U-shaped plate is put into the O-press and formed into an O shape by the upper and lower dies. The two edges are butted against each other, tack welded, and then subjected to submerged-arc welding, one layer on the inside and the other on the outside.

After that, the expander radially expands circumferentially divided segments set on the inside of the pipe until the pipe cross section is almost perfectly round. If the finished pipe is to be used as a line pipe, it is subjected to anti-corrosion coating at 200˚C to 250˚C at the construction site or in the manufacturing plant. UOE pipes manufactured using the above process are girth welded into a pipeline at the construction site.

2.2 Strain-based design of pipeline

The representative load condition for line pipes laid in discontinuous permafrost regions to which SBD is applied is the bending moment under internal pressure, and the typical failure modes are local buckling due to a compressive stress in the intrados and ruptures (ductile fractures) caused by the tensile stress in the extrados. Ordinarily, local buckling precedes the rupture, and hence, the strain that initiates a local buckling is assumed to be the compressive strain limit. Therefore, it is necessary that the compressive strain limit should be above the strain demand. On the other hand, the tensile strain limit takes a value not greater than the strain that initiates a rupture and not smaller than the compressive strain limit. It is determined from the dimensions of the girth weld defects by any of the various approaches based on fracture mechanics. Therefore, in the present study, we analyzed the buckling behavior of a UOE pipe under a bending with an internal pressure focusing on the compressive strain limit.

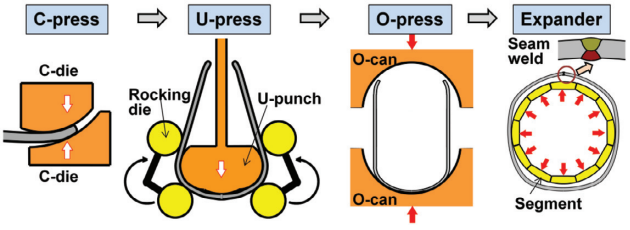

Fig. 1 Summary of UOE pipe forming process

3. Role of Numerical Simulation in Problem Solving

3.1 Study of forming of high-strength UOE pipe

When forming a high-strength steel plate into a UOE pipe using the process shown in Fig. 1, if the bending work by the U-press is insufficient because of a large spring back, the steel plate cannot be properly set in the succeeding O-press. Insufficient upset in the O-press produces an excessive seam gap between the edges, thereby exerting an adverse effect on the quality of the tack weld. Besides, there are concerns that the use of a high-strength steel plate requires larger capacity presses. Solving those problems requires techniques to control the spring back and press load for different pipe sizes and different material strengths. This, together with the interaction between presses, makes it extremely difficult to optimize the UOE pipe-forming process by experimentation with actual pipe-forming equipment from the standpoint of maintenance of the production equipment as well. In this respect, the high-precision numerical simulation of steel pipe forming is an effective tool when developing new UOE pipes.

3.2 Study of the performance properties of steel pipe

3.2.1 Plastic anisotropy of a UOE pipe

Fig. 2 shows the stress-strain (SS) curves obtained with an X80 UOE pipe 914 mm in diameter and 19.8 mm in wall thickness. For the SS measurement, round bar specimens (ϕ = 8.9 mm) collected in the longitudinal (L) and circumferential (C) directions from a position 45˚ away from the seam were used. The SS curves were obtained from the pipe as formed and from the pipe heated at 240˚C for 5 minutes simulating the heating conditions for anti-corrosion coating. The SS curve of the pipe as formed is round in the L direction and rectangular in the C direction. Thus, the pipe as formed shows the so-called orthogonal anisotropy; that is, the shape of the SS curve in the L direction is different from that in the C direction. This orthogonal anisotropy is due to the application of tensile stress in the C direction—the maximum principal strain direction—by the expander in the final step of the UOE pipe-forming process. After the heating, both the yield strength (YS) and tensile strength (TS) in the L and C directions increase as a result of strain aging. While the shape of the SS curve in the L direction remains round, a yield point elongation (YPE) of as much as 2% appears after the upper yield in the C direction, whereby the work-hardening anisotropy of the pipe as formed is further intensified by heating.

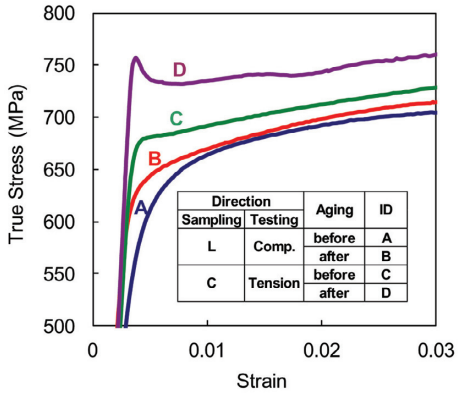

Fig. 2 SS curves for UOE pipe

It is difficult to independently control the SS curves in the L and C directions experimentally. Therefore, we had not been able to quantify the influence on the steel pipe-buckling behavior of the characteristics of the SS curves in the L direction—the principle stress direction under bending—and in the C direction that intersects the L direction orthogonally.

3.2.2 Analysis of steel pipe performance used in SBD

The factors that govern the buckling of a steel pipe under bending can approximately be divided into material factors and form factors. A certain variation in strength is allowed for steel pipes that are manufactured on a commercial basis. This means that the steel pipes that are girth welded together at the construction site may have a difference in strength within the prescribed limit. In the plastic design of a steel pipe, it is necessary to consider such strength variations of each individual pipe as well.

As form factors, not only the geometric imperfection inherent in the steel pipe in the UOE-forming process, but also deformation caused by the residual stress in girth welding and the offset (misalignment) during butt welding, etc. may be cited.

To quantify the above material and form factors, the numerical simulation technique that has been validated by the testing of actual steel pipes is very effective.

4. Method of Simulating Steel Pipe Forming and Performance

To conduct a highly accurate simulation of steel pipe forming and performance based on FEA, it is necessary to apply the appropriate material constitutive law and pipe-forming models. The simulation method is described below.

4.1 Material constitutive law

4.1.1 Model for forming analysis

For the FEA model of pipe forming, which was intended to accurately predict the spring back, the proven yield functions of Teodosiu-Hu were used.[1)] Thus, to determine the parameters for the model, we carried out tensile and compression tests using round bar specimens.

4.1.2 Model for flexural buckling analysis

In the case of a UOE pipe heated for anti-corrosion coating, unlike a UOE pipe as formed, YPE manifests itself in the SS curve in the C direction, whereas the SS curve in the L direction remains round (Fig. 2). This change in the SS curve due to the heat treatment cannot be considered using the conventional material constitutive law, and hence, a consistent simulation for the analysis of pipe forming and performance cannot be implemented. Therefore, we attempted to build a new material constitutive law with the characteristics of a steel pipe after heat treatment assumed as the initial material characteristics.

For a material constitutive law that permits the consideration of anisotropies, Hill's quadratic yield functions shown in the following equations were used as the base.

$$f = J(\boldsymbol{\sigma}, \mathbf{n}_i, \bar{\varepsilon}) - g_{11}(\bar{\varepsilon}) = 0 \tag{1}$$

$$J(\boldsymbol{\sigma}, \mathbf{n}_i, \bar{\varepsilon}) = \left[\frac{1}{2}\left\{H_F\left(\hat{\sigma}_{22}-\hat{\sigma}_{33}\right)^2 + H_G\left(\hat{\sigma}_{33}-\hat{\sigma}_{11}\right)^2 + H_H\left(\hat{\sigma}_{11}-\hat{\sigma}_{22}\right)^2 + H_L\hat{\sigma}_{12}^2 + H_I\hat{\sigma}_{23}^2 + H_K\hat{\sigma}_{31}^2\right\}\right]^{1/2} \tag{2}$$

$$\hat{\sigma}_{ij} = \mathbf{n}_i \cdot \sigma \cdot \mathbf{n}_j \tag{3}$$

where σ denotes Cauchy stress; $\mathbf{n}_i$ denotes unit vector in the normal direction along orthogonal coordinate $\hat{x}_i$; $\bar{\varepsilon}$ denotes equivalent plastic strain; J denotes equivalent stress; and g_{11} denotes work-hardening function in uniaxial tensile test along $\hat{x}_1$. In their application to a steel pipe, $\hat{x}_1$, $\hat{x}_2$, and $\hat{x}_3$ were assumed to be in the L direction, C direction, and wall thickness (t) direction, respectively. H_F–H_K are orthogonal coefficients for considering anisotropies. To express anisotropic work hardening, the orthogonal coefficients were defined as functions of equivalent plastic strains. For the purpose of simplification, H_I and H_K were assumed to be 6 and the stress-strain behaviors in $\hat{x}_1$ and $\hat{x}_3$ were assumed to be the same. By using g_{11}, g_{22}, g_{33}, and g_{45}, which are the functions of work hardening by uniaxial tension in $\hat{x}_1$, $\hat{x}_2$, $\hat{x}_3$, and the direction 45° from $\hat{x}_1$, all the orthogonal coefficients are calculated using the following equations.

$$H_F = \frac{1}{\Sigma_{22}{}^2}, \quad H_G = -\frac{1}{\Sigma_{22}{}^2} + 2, \quad H_H = \frac{1}{\Sigma_{22}{}^2} - 2,$$
$$H_L = \frac{8}{\Sigma_{45}{}^2} - 2, \quad H_I = 6, \quad H_K = 6 \tag{4}$$

$$\Sigma_{22} = \frac{g_{22}(\bar{\varepsilon})}{g_{11}(\bar{\varepsilon})}, \quad \Sigma_{45} = \frac{g_{45}(\bar{\varepsilon})}{g_{11}(\bar{\varepsilon})} \tag{5}$$

H_F–H_K are orthogonal coefficients and parameters representing anisotropies. Ordinarily, the orthogonal coefficients are handled as constants that represent the anisotropy of yield strength or anisotropy of the r-value (Lankford value). However, in the strain region in which YPE appears in the SS curve in the C direction after strain aging, the work hardening coefficient differs markedly between the L and C directions and the yield surface does not expand analogously. Thus, by converting the orthogonal coefficients into strain functions, the yield surface expands while changing its form. In the present study, this anisotropic yield function shall be referred to as Hill's modified yield function (m-Hill).

4.2 Model for the demonstration of the material constitutive law

The MARC—FEA universal code—was used for the FEA model of a steel pipe. The yield functions of Teodosiu-Hu and Hill (m-Hill) were built in hypela2—one of the user subroutines of MARC—to calculate the equivalent stress and equivalent plastic strain and obtain the expansion and movement of the yield surface. To demonstrate the model, we used one eight-node solid element.

4.3 FEA model of UOE pipe forming

Fig. 3 shows an FEA model of minipress test apparatus in a form similar (scale: 1/7) to actual UOE manufacturing equipment. The model consists of a stock plate, C-press (upper and lower C dies), U-press (U-punch and rocking die), O-press (upper and lower O-can), and expander (expansion segments). The seam weld was modeled by sequentially making the inner and outer surfaces an active element, and an unsteady thermal-stress analysis was carried out as-

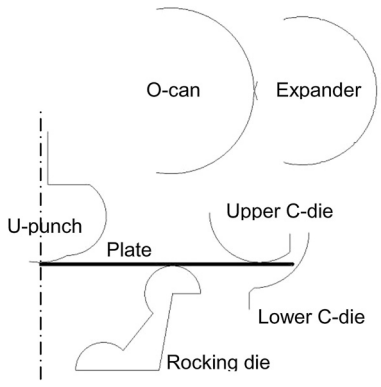

Fig. 3 FEA model for UOE pipe forming

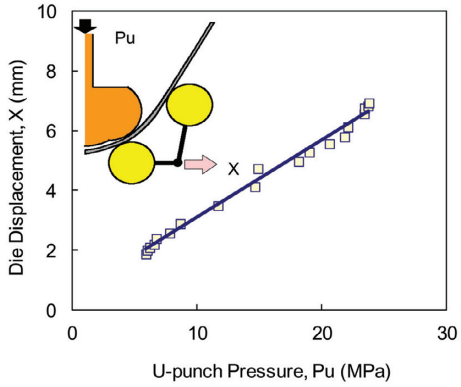

Fig. 4 Relationship between U punch pressure and rocking die displacement

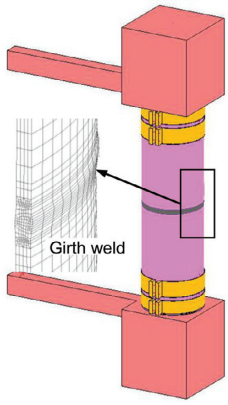

Fig. 5 FEA model for bending of girth-welded pipes

suming the cooling of the pipe from 1,300˚C. A plane strain element was used as the stock plate, and a large-deformation elastic-plastic analysis using the yield function of Teodosiu-Hu was performed. Rigid elements were used for the dies, and the forming of the stock plate by the dies was treated as a contact problem.

The final die positions are determined on the basis of load control for the C-press and displacement control for the U-press, O-press, and expander. The basic driving force of the U-press is the U-punch load, and the rocking die rotates under a vertical thrust from the U-punch. At this moment, the plate winds on the U-punch and is formed into a U shape. The rocking die is capable of helping the U-punch operation since extra moment is applied to it from a side cylinder.

In actual UOE pipe-manufacturing equipment, a phenomenon can be observed whereby dies "run off" during the press operation caused by the insufficient rigidity of the housing of the apparatus. This phenomenon does not occur in the FEA since the dies are modeled as rigid bodies. Therefore, we measured the displacement of the center of rotation of the rocking die in actual UOE pipe-manufacturing equipment.

Fig. 4 shows the U-punch main cylinder pressure and the horizontal displacement at the center of the rocking die rotation. The rocking die moves outward as the cylinder pressure or the punch load is increased. Therefore, we decided to simulate the run-off of the die by placing a spring at the center of the rocking die on the pipe-forming model with the inclination in Fig. 4 used as the spring constant.

4.4 FEA model of the bending of a girth-welded steel pipe

Fig. 5 shows an FEA model for bending tests of actual girth-welded steel pipes. The girth-welded part was positioned in the center of the model, and the geometric imperfections of the steel pipe and welded joint were reflected by those in the L- direction measured by a laser displacement gauge. For the material model, the yield function m-Hill was used with the SS curves in the C and L directions shown in Fig. 2 as the initial values.

Table 1 shows the simulation conditions for bending in comparison with experimental conditions. For each of the three pipes tested, isotropic hardening (ISO) using Mises' yield function and anisotropic hardening (ANISO) using m-Hill were assumed and the influence of the hardening law on the pipe-buckling behavior was evaluated. As in the tests using actual pipes, a specified minimum yield stress (SMYS) of 72% was applied to the pipe body first and then the bending load was applied to the arm of the pipe body endplate.

Table 1 Experimental and numerical conditions for pipe bending

Case	Experimental condition				Numerical model	
	Pipe No.	Girth weld	Heating temp.(˚C)	Internal pressure	Type of SS curve	Yield function
A	1	None	None	72% SMYS	As formed	ISO ANISO
B	2	None	240		Aged	
C	3	With	240		Aged	

5. Experimental Method

5.1 Testing for the demonstration of the material hardening law

For demonstrating the FEA model that uses the yield functions of Teodosiu-Hu and m-Hill, we carried out a compression-tension cyclic loading test,[2] and a biaxial loading test[3] using round-bar specimens (ϕ = 5 mm) and cruciform specimens (260 mm × 260 mm × 1.8 mm), respectively. The round-bar specimens were collected from X80, X100, and X120 steel plates and subjected to compression-tension cyclic loading of ± 2%, ± 4%, and ± 6%. The cruciform specimens were collected from an X80 steel sheet. In the biaxial loading test, after a 2% tensile prestrain was applied to the X axis, biaxial stresses that made the stress ratio of the X and Y axes 1:2, 1:1, and 2:1 were applied to the specimens.

5.2 Minipress experiment for forming a UOE pipe

To determine the validity of the UOE pipe-forming simulation model on actual manufacturing equipment, consideration must be given to the equipment alignment, wear, housing rigidity, and material strength distribution, etc. However, they can barely be reflected in the FEA model precisely. Therefore, we decided to judge the validity of the numerical analysis model using a press test ("minipress") with 1/7-scale dies that have a shape similar to that of the actual equipment.

Fig. 6 shows the minipress equipment consisting of C, U, and O-presses and an expander. The experiment was carried out on a 1/7 scale for 1,219 mm OD, 19 mm t. The dies were set in a 3,900-kN universal press. As stock plates, high-strength line pipe materials cut from X80, X100, and X120 steel plates were used.

5.3 Pipe bending test

To evaluate the buckling behavior under internal bending pressure, the test was carried out with actual pipes by using the universal test apparatus of C-FER Technology (Canada).[4] The test conditions

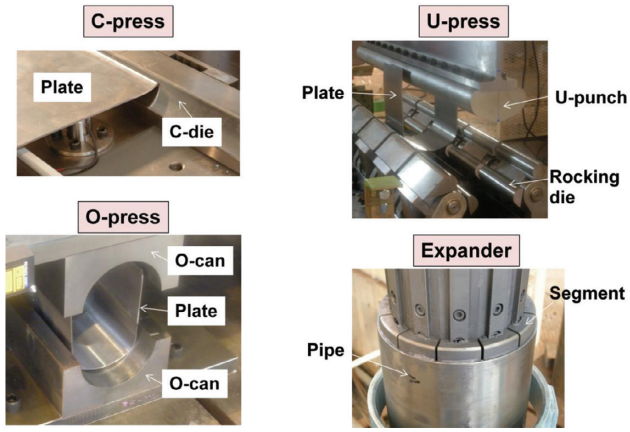

Fig. 6 Testing apparatus for minipress

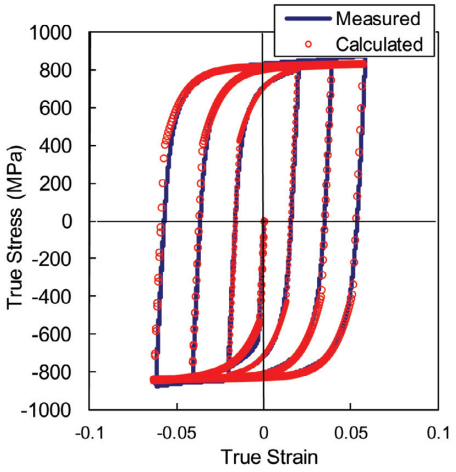

Fig. 7 Comparison of plastic hysteresis between experiment and FEA

are shown in Table 1. As the form factor for a UOE pipe, the geometric imperfection of the pipe itself and the girth weld was studied. As the material factor, while the SS curves in the L direction were all round, as-formed materials whose SS curves in the C direction did not contain YPE and heated materials containing YPE were selected. The bending strain was obtained by the following equation from the bending angle measured by an inclinometer installed on the neutral axis at intervals of 1 D.

$$\varepsilon_{bend} = \frac{\theta}{2\Delta L / D} = -\varepsilon_{neutral} - \varepsilon_0 \qquad (6)$$

where ε_{bend} denotes bending strain; $\varepsilon_{neutral}$, strain at the neutral axis; ε_0, strain under internal pressure load; θ, bending angle (rad); ΔL, gauge length (mm); and D, outside diameter (mm). In the present experiment, ΔL was assumed to be 1 D. The compressive strain limit, ε_{Limit}, at which local buckling occurs was defined as ε_{bend} at the time the bending moment reaches its maximum value.

6. Prediction of the Plastic Deformation Behavior by FEA

Fig. 7 shows the plastic hysteresis calculated by the FEA using the yield function of Teodosiu-Hu and the results of a compression-tension cyclic loading test using round-bar specimens of X100. With ± 6% strains, the second and third yields are accurately approximated.

Fig. 8 shows the stress-strain behavior under biaxial loading calculated by the FEA using the m-Hill yield function, together with the results of a biaxial loading test using cruciform specimens of X80. The figure also shows the results of calculations using Mises' yield function—a representative yield function for isotropic materials. In the figure, the plastic strain on the X-axis was defined as the amount of strain beyond the proportional limit on the SS curve. Under equibiaxial stress loading under which the stress ratio between the X- and Y-axis ($\sigma_x : \sigma_y$) is 1:1, the results of calculations using the above yield functions agree well with the measurement results. However, when $\sigma_x : \sigma_y$ = 1:2, or when the direction of maximum principal strain so inclines as to orthogonally intersect the pre-strained direction, the measured yield point is much lower than when $\sigma_x : \sigma_y$ = 1:1 or 2:1. While the calculation using Mises' function overestimates the yield point, the calculation result using m-Hill agrees well with the measurement result.

The above results of the minipress test validated the yield functions used in simulations of actual UOE pipes.

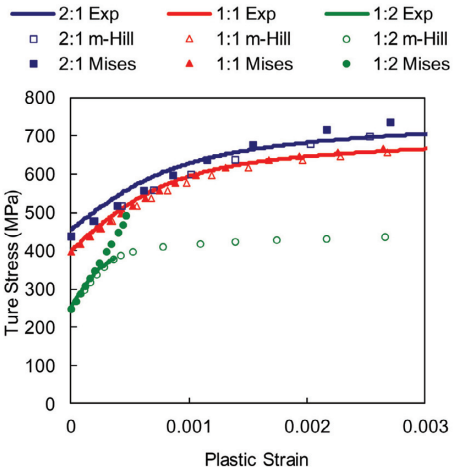

Fig. 8 SS curves under biaxial loading

7. Results of the Simulation of UOE Pipe Forming

The major problems involved in forming pipes from high-strength steel plates are the strong spring back of the plate after the press operation and the need for presses having a larger capacity. In this paper, we discuss the above two problems on the basis of results of numerical analysis and experimentation and present guidelines on the technology for forming high-strength steel pipes.

7.1 Spring back during steel pipe forming and operational guidelines

7.1.1 U width after U-press operation

Fig. 9 shows the results of the minipress test with a 1/7-scale FEA model in terms of the relationship between U-punch stroke and U width. Here U width means the maximum amount of opening in U after the U-press operation. With the increase in U-punch stroke, the U width decreases inversely. The figure also suggests that the higher the steel strength is, the larger the required U-punch stroke. Since the values obtained by the FEA agree well with the experimental values, in the U-press in which the strain increases monotonously,

we could demonstrate that the model can accurately predict the amount of spring back. Therefore, even with an ultrahigh-strength steel such as X120, the FEA permits calculating the optimum U-punch stroke for inserting the U-shaped plate into the O-press.

Fig. 10 shows the relationship between the U width and U-punch displacement from the reference point in the forming of X120 pipe 1,219 mm in outside diameter and 19 mm in wall thickness. It shows the FEA results obtained with the rocking die fixed and with the rocking die moved according to a measured spring constant. From the figure, it can be seen that when the rocking die is fixed as in the mini-press, the decrease in the U width is overestimated so much as to make the FEA result useless. By contrast, when the movement of the rocking die is considered in the spring model, the FEA result agrees well with the experimental result.

Thus, we could establish a technique to determine the optimum U width of the stock plate to be inserted into the O-press in actual pipe forming equipment by FEA.

7.1.2 Seam gap after O-press operation

Fig. 11 shows the relationship between O-can displacement and seam gap. Here the O-can displacement means the relative displacement from the position at which the upset rate (i.e., the amount of mean compressive plastic strain around the circumference)—index of O-press forming—becomes zero. It can be seen that there is only a weak correlation between O-can displacement and seam gap but that the influence of plate strength on the seam gap is significant.

With X120, in particular, the widening of the seam gap is conspicuous. An excessive seam gap should be avoided since it causes defective tacking during seam welding. In the case of X120, the seam gap cannot sufficiently be narrowed by the effect of upset rate alone, and hence, it is necessary to utilize the synergism with the U width. On the other hand, excessive upset has induced very serious damage known as edge buckling in X80. Therefore, it is necessary to obtain the optimum upset rate in accordance with the steel strength. For all the steel grades under consideration, the experimental results and FEA results agree well, suggesting that even in the O-press in which the stock plate is subject to bending and re-bending, the FEA model is an effective tool for obtaining the optimum upset and combined effect between presses.

7.1.3 Effect of correcting pipe ovality by expander

Fig. 12 shows the ovality of a 1/7-scale model of an X120 pipe 1,219 mm in outside diameter and 19 mm in wall thickness before and after expansion by an expander. The ovality, β, is expressed by the following equation.

$$\beta\,(\%) = \left(D_{\max} - D_{\min}\right) / D_{ave} \times 100 \qquad (7)$$

where D denotes the outside diameter of the pipe. The ovality of a steel pipe affects the reduction of the misalignment of girth welding performed at the pipeline construction site. The less the ovality, the better it is. Expanding the pipe is the final step in the UOE-pipe-forming process. It can be understood that increasing the pipe expansion rate minimizes the ovality of the finished product. On the other hand, the pipe expansion rate has a positive correlation with

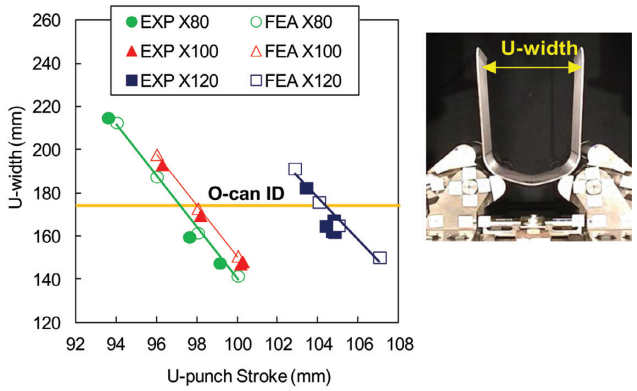

Fig. 9 Relationships between U punch stroke and U width

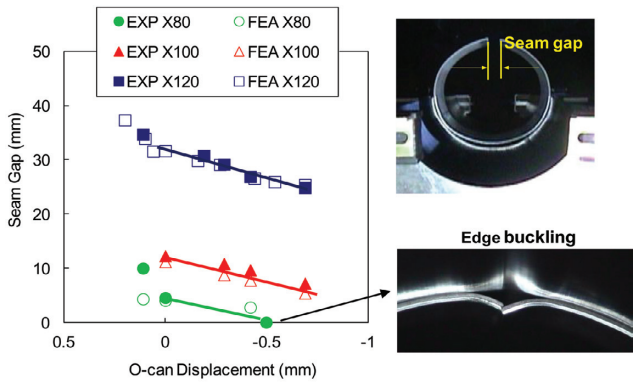

Fig. 11 Relationships between O can displacement and seam gap

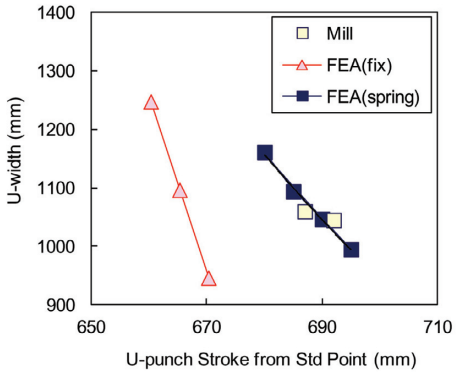

Fig. 10 Relationships between U punch stroke and U width for full scale mill

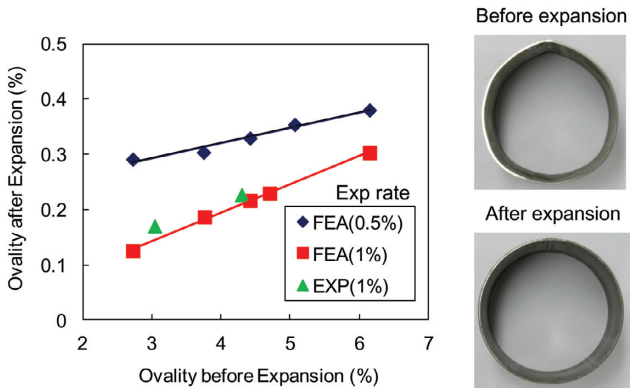

Fig. 12 Ovality before and after expansion

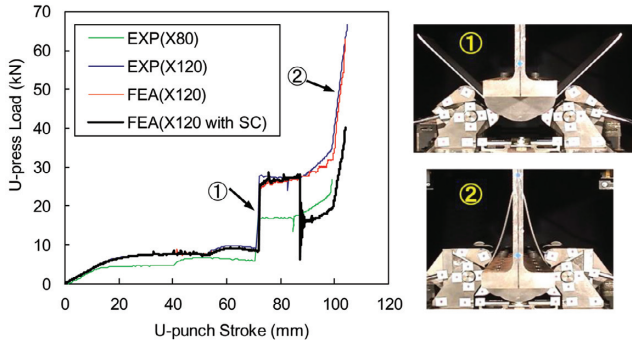

Fig. 13 Loading behavior during U press

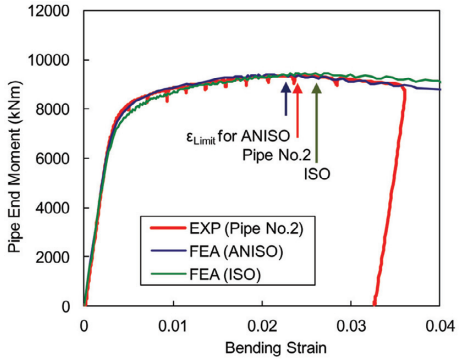

Fig. 14 Bending moment vs. strain curves

the ovality of the pipe before expansion. Thus, the results shown in Fig. 12 suggest that optimum tooling not only in the pipe expansion process, but also in the C, U, and O-presses is effective to minimize the ovality of the pipe.

7.2 Prediction of forming load and application of FEA in equipment design

Fig. 13 shows the U-punch loading behavior on X80 and X120 in the minipress test and the loading behavior on X120 in the FEA analysis with and without a side cylinder. The punching load on X120 is characterized by a sharp increase indicated by ① and ② in the figure. It can be seen that the increase indicated by ① occurs when the rocking die begins to turn and that the increase indicated by ② occurs when the plate edges make contact with the punch bar. The loading behavior on X80 shows a hysteresis similar to that on X120, but its absolute value decreases to half with a decrease in steel strength. When forming X120 into a UOE pipe, it might become necessary to employ a larger capacity U-press.

In considering the solution to the above problem, we applied a numerical simulation. A comparison between the experimental and FEA results obtained with X120 shows that both the absolute loads and load behaviors agree well. In the FEA provided with the side-cylinder function, a rotating circumferential load is produced when the rocking die rotation reaches a certain value. At that moment, the main cylinder load decreases to half, and the ultimate load can also be reduced substantially. Since, in the actual pipe-forming equipment, the main cylinder pressure is interlocked with the side-cylinder pressure that applies the circumferential load, it is possible to form even high-strength stock plates with the existing press capacity.

8. Simulation Results of UOE Pipe Bending

In this chapter, we describe the results of our numerical simulation of the influence of the orthogonal anisotropy of a UOE pipe on the buckling behavior.

8.1 Accuracy of prediction of flexural buckling limit

Fig. 14 shows the bending moment-strain curve obtained with Pipe No. 2. The strain was calculated as the bending strain in Equation (6). The figure also shows the bending moment behaviors calculated using the yield functions of m-Hill (indicated by ANISO) and Mises (indicated by ISO), respectively. After the bending moment reaches its maximum, local buckling begins to progress rapidly. Therefore, the bending strain at the maximum bending moment is defined as the compressive strain limit, ε_{Limit}. A comparison of ε_{Limit} between the experiment and FEA shows that ISO overestimates ε_{Limit}.

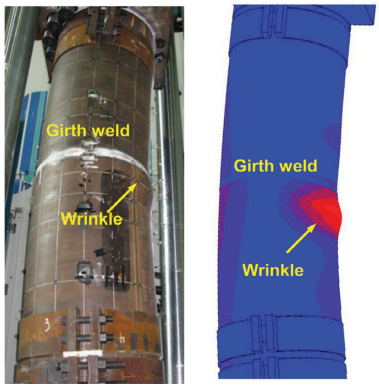

Fig. 15 Local buckling during bending test

On the other hand, ANISO predicts the experimental value accurately. Comparing the yield points, the moment behavior by ISO is rounder than the experimental or ANISO value, which implies that the yield elongation and high yield strength of the SS curve in the C direction cause the flexural deformability to deteriorate and push up the yield point simulataneously.

Fig. 15 compares the deformation of Pipe No. 3 after the progress of local buckling between the experiment and simulation using ANISO. The experiment and FEA show the same local buckling occurrence points. This, together with the moment behavior shown in Fig. 14, has clarified that by using m-Hill, it is possible to accurately predict the buckling behavior of a UOE pipe that has orthogonal anisotropy.

Fig. 16 compares ε_{Limit} for three pipes between the experiment and FEA using ANISO and ISO. For as-formed Pipe 1, the error in prediction is relatively small even with ISO. , However, for Pipe 2, the prediction error increases for the reason mentioned above, and the prediction error of Pipe 3 becomes still larger. The latter is considered to be caused by at least in part, to the influence of the hardening law and the fact that local buckling occurred at a point on the upper pipe shown in Fig. 14.

8.2 Influence of orthogonal anisotropy on the buckling behavior of the steel pipe

Fig. 17 shows the results of an ANISO/ISO analysis of the influence of the pipe's internal pressure on ε_{Limit}. As has been suggested by previous studies, the analysis results show that ε_{Limit} increases with the internal pressure load. In a low-pressure region below 40%

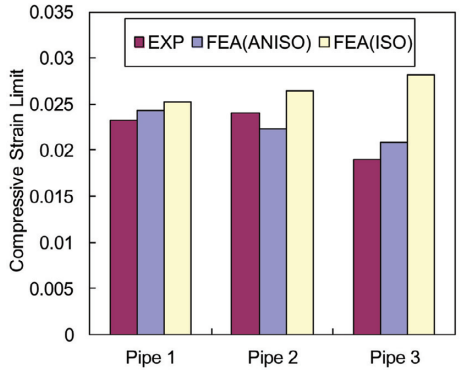

Fig. 16 Comparison of ε_{Limit} between experiment and FEA

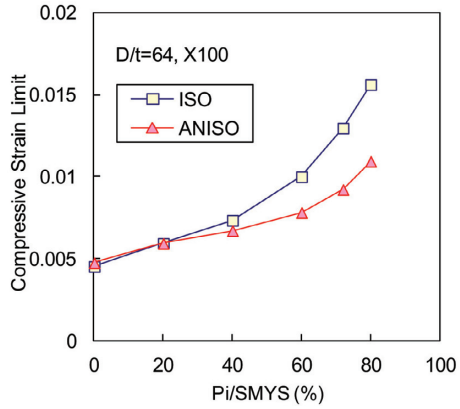

Fig. 17 Effect of internal pressure on ε_{Limit}

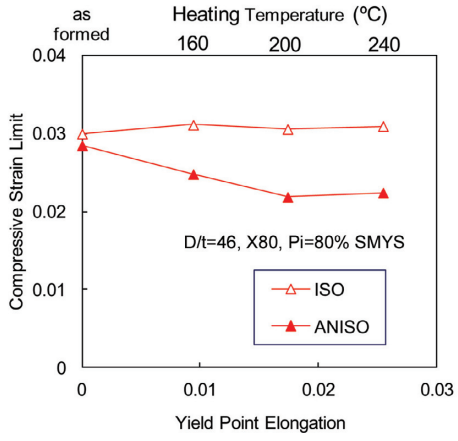

Fig. 18 Effect of YPE on ε_{Limit}

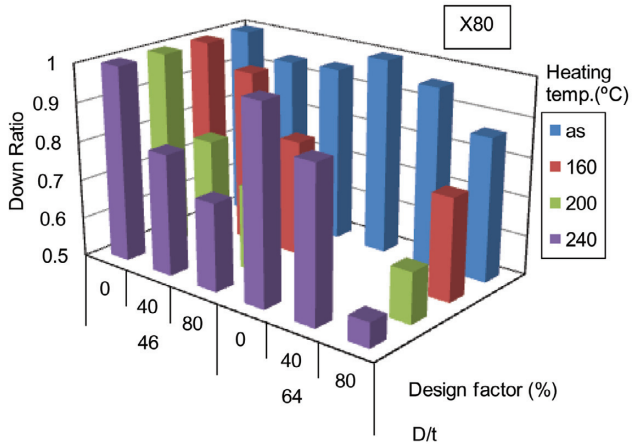

Fig. 19 Reduction ratio of ε_{Limit} by plastic anisotropy

SMYS, there is no significant difference in ε_{Limit} between ANISO and ISO. However, it was found that with a high design factor (above 72% SMYS) applied in SBD, there is the risk that ε_{Limit} would be overestimated when the conventional isotropic hardening law is used.

On the other hand, as long as the SS curve in the C direction has become round, it does not cause ε_{Limit} to decrease even under a high internal pressure. **Fig. 18** shows the relationship between C direction YPE and ε_{Limit} under 80% SMYS, obtained with the X80 UOE pipe with D/t = 46. On the secondary X-axis, the heating temperature corresponding to YPE is shown. It can be seen that when YPE begins to occur at the heating temperature of 160˚C, ε_{Limit} starts decreasing, but that the rate of decrease in ε_{Limit} almost levels off after YPE reaches approximately 2% at 200˚C.

The influence of YPE on ε_{Limit} depends not only on the YPE value, but also on the D/t and internal pressure. Therefore, it is necessary to quantify it in each individual project. **Fig. 19** shows the decreases in ε_{Limit} calculated by ANISO and ISO when the influence of the C direction SS curve is considered. It may be said from the figure that the rate of reduction of ε_{Limit} increases as a higher design factor is applied to pipes with a smaller wall thickness. Such a pipe design is applied to long-distance gas pipelines. In discontinuous permafrost regions and other similar environments in which SBD is applied, evaluating the influence of the C direction SS curve is considered very important.

In determining the ε_{Limit} in conventional SBD, the performance limit has been predicted using a numerical simulation technique proven by actual pipe tests and considering the prescribed strength range. In the present study, through the development of a new yield function that permits defining the orthogonal anisotropy of work hardening, we clarified the influence of the C direction SS curve on the flexural buckling behavior of a steel pipe. This will help improve the reliability of SBD.

9. Conclusion

When forming a high-strength UOE pipe, poor formability due to excessive spring back and the need to use presses of larger capacity can become problematic. In addition, in the case of UOE line pipes, the manufacturing process and the application of a model of orthogonal anisotropy caused by heating for anti-corrosion coating had been key in the analysis of pipe-buckling behavior. The results of the present study are summarized below.

(1) By applying the yield function of Teodosiu-Hu to the general-purpose FEA program in the forming of a UOE pipe which is repeatedly subjected to bending and bending-back, we could establish a highly accurate numerical simulation method.

(2) A spring constant was introduced to express the rigidity of press housing to apply a forming model to actual UOE pipe manufacturing equipment. As a result, the model became an effective

tool for analysis.

(3) The numerical simulation described above has made it possible to determine the optimum conditions for forming high-strength steel materials and guidelines on equipment improvement.
(4) We proposed an improved version of Hill's yield function (m-Hill) that permits considers work-hardening anisotropy that is observed in UOE pipe after heating for anti-corrosion coating.
(5) The pipe-bending FEA model using m-Hill has clarified that the yield elongation appearing on the C direction SS curve causes the flexural buckling limit to decrease.
(6) The influence of the C direction yield elongation on buckling depends on the steel pipe size and internal pressure. Preparing a diagram of their correlation helps improve the reliability of SBD.

References

1) Suzuki, N. et al.: Advanced Constitutive Model for Spring Back Prediction of High Strength Steel Sheet. Journal of the Japan Society for Technology of Plasticity. 46 (536), 636-640 (2005)
2) Tsuru, E. et al.: Numerical and Experimental Evaluation of Formability and Buckling Resistance for High Strength Steel UOE Pipe. The 159th ISIJ Spring Meeting. Vol. 23, p. 297-300
3) Tsuru, E. et al.: Numerical Simulation of Buckling Resistance for UOE Line Pipes with Orthogonal Anisotropic Hardening Behavior. Proc. of 2008 Int. Offshore and Polar Engineering Conf. ISOPE, p. 104-110
4) Tsuru, E., Agata, J.: Buckling Resistance of Line Pipes with Girth Weld Evaluated by New Computational Simulation and Experimental Technology for Full-Scale Pipes. Proc. of 2009 Int. Offshore and Polar Eng. Conf. ISOPE, p. 204-211

Eiji TSURU
Chief Researcher, Dr.Eng.
Plate, Pipe, Tube & Shape Research Lab.
Steel Research Laboratories
20-1, Shintomi, Futtsu, Chiba 293-8511

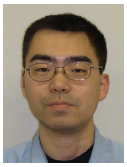

Jun AGATA
Senior Researcher
Plate, Pipe, Tube & Shape Research Lab.
Steel Research Laboratories

Yukinobu NAGATA
Researcher, Dr.Eng.
Plate, Pipe, Tube & Shape Research Lab.
Steel Research Laboratories

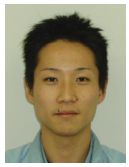

Satoshi SHIRAKAMI
Researcher
Forming Technologies R&D Center
Steel Research Laboratories

Yasuhiro SHINOHARA
Senior Researcher
Plate, Pipe, Tube & Shape Research Lab.
Steel Research Laboratories